Dynamics of Drag and Force Distributions for Projectile Impact in a Granular Medium

Massimo Pica Ciamarra,[1,2,*] Antonio H. Lara,[1] Andrew T. Lee,[1] Daniel I. Goldman,[1]
Inna Vishik,[1] and Harry L. Swinney[1,†]

[1]*Center for Nonlinear Dynamics and Department of Physics, University of Texas at Austin, Austin, Texas 78712, USA*
[2]*Dipartimento di Scienze Fisiche, Universitá di Napoli "Federico II" and INFM, Unitá di Napoli, 80126 Napoli, Italia*

(Received 7 November 2003; published 14 May 2004)

Our experiments and molecular dynamics simulations on a projectile penetrating a two-dimensional granular medium reveal that the mean deceleration of the projectile is constant and proportional to the impact velocity. Thus, the time taken for a projectile to decelerate to a stop is independent of its impact velocity. The simulations show that the probability distribution function of forces on grains is time independent during a projectile's deceleration in the medium. At all times the force distribution function decreases exponentially for large forces.

DOI: 10.1103/PhysRevLett.92.194301 PACS numbers: 45.70.–n, 45.50.–j, 89.75.Da, 96.35.Gt

Craters on the Earth and the Moon are similar to craters formed in laboratory experiments at much lower energies by using projectiles and explosives [1–3]. In laboratory experiments at large impact energies, narrow jets have been observed to rise even higher than the initial height of the projectile [4,5]. Recent experiments have determined how the shape, depth, and width of craters formed in granular media depend on the energy of the impact projectile [6,7], but there is little known about the dynamics of a projectile during crater formation.

We have studied the time evolution of projectile motion. Our experiments and molecular dynamics simulations on a two-dimensional granular medium yield the time dependence of the drag force on projectiles. Simulations for the same conditions are in accord with the experiment and also yield the time evolution of the forces on all of the particles; hence, we can study the time dependence of the force probability distribution function at different stages of the projectile motion.

Our observations and simulations reveal three distinct regimes of the motion, as illustrated in Fig. 1: *impact,* where the projectile first hits the granular medium; *penetration,* where a transient crater forms and grains in front of the projectile are fluidized; *collapse,* where the projectile has almost stopped and the deep transient crater collapses, forming a static crater that remains visible on the surface.

Methods.—In the experiment, a projectile of diameter $D = 4.46$ cm and mass 32.2 g was dropped into a bed of small particles (cylinders) contained between two glass plates with a separation 1.1 times the length of the cylinders. The initial projectile heights h ($h < 80$ cm) correspond to impact velocities up to 400 cm/s. To reduce crystallization, two sizes of small particles were used: 12 600 particles (84% of the total number) had diameter $d_1 = 0.456$ cm (mass $m_1 = 0.049$ g) and 2400 particles had diameter $d_2 = 0.635$ cm (mass $m_2 = 0.097$ g). To obtain a uniform granular bed with a reproducible area fraction before each drop of the projectile, the bed was fluidized with air flow that was slowly reduced to zero, yielding the same bed height ($65d_1$) and area fraction [$(81 \pm 2)\%$] for each projectile drop. The bed width was $225d_1$. The position of the projectile, $y(t)$, defined as the distance between the bottom of the projectile and the initial height of the bed, was determined with a high speed camera and a center of mass particle tracking algorithm [8].

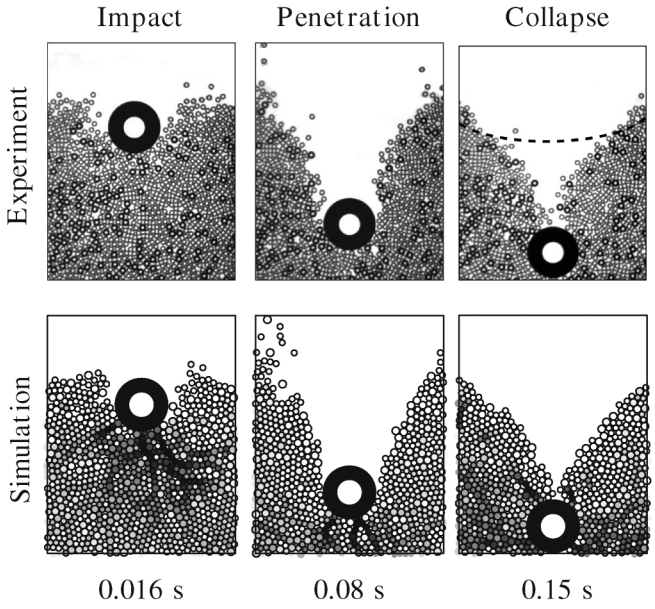

FIG. 1. Snapshots of a projectile in the three distinct regimes of its motion in a bidisperse mixture of particles (cylinders). Experiment: the larger cylinders of the bidisperse mixture are colored black for visualization and are 40% larger in diameter than the grey cylinders. The dashed line shows the location of the surface after the collapse is complete. Simulation: the shading of each particle is proportional to the sum of the magnitudes of all the normal forces acting on that particle; this renders visible the instantaneous force chains. The projectile is 9.8 times as large in diameter and 657 times as massive as the smallest particles.

We modeled the system with a soft-core molecular dynamics (MD) simulation that used 15 000 disks that had the same sizes and area fraction as the experiment. Any two disks (one of which can be the projectile) exert the following normal and tangential forces on one another:

$$\vec{F}_n = -[k\delta + m_r\gamma_n|\vec{v}_n|\theta(\vec{v}_n)]\hat{n}, \quad (1)$$

$$\vec{F}_s = \min[m_r\gamma_s|\vec{v}_s|, \mu|\vec{F}_n|]\hat{s}, \quad (2)$$

where δ is the length of overlap [9,10], and $\vec{v}_n$ and $\vec{v}_s$ are, respectively, the normal and the tangential component of the surface velocity ($\hat{n}$ and $\hat{s}$ are unit vectors parallel to $\vec{v}_n$ and $\vec{v}_s$). The four parameters of the model were found empirically for one impact velocity, and the same parameters were used for all other simulations: $k = 3.2 \times 10^3$ kg s^{-2} [11–14] is proportional to Young's modulus, $\gamma_n = 10^4$ s^{-1} and $\gamma_s = 8 \times 10^3$ s^{-1} are viscoelastic constants, and $\mu = 0.28$ is the static friction coefficient. m_r is the reduced mass ($m_r^{-1} = m_A^{-1} + m_B^{-1}$ for two particles A and B). The Heaviside function θ in $\vec{F}_n$ models an elastic-plastic interaction (e.g., see Fig. 8 of [15]); the use of the Heaviside function distinguishes our force model from previous soft-core MD simulations [9,14]. Simulations with a more realistic form for $\vec{F}_s$ [16] yielded results not significantly different from our simple form, which is computationally more efficient. A comparison of the simulation output using time steps shorter than 1 μs did not yield different results; a 1 μs time step was used in the results presented here.

Results.—The simulation results agree remarkably well with the laboratory observations, as Fig. 2 illustrates. Both experiment and simulation reveal that the time taken for a projectile to slow to a stop in the granular medium is *independent* of its velocity at impact. The large deceleration of the projectile at impact (see Fig. 3) is similar to that of a projectile incident on a liquid. However, in contrast to the behavior of a projectile in a fluid [17], in the granular medium there is a long penetration region in which the projectile's average acceleration is constant: $y(t)$ is described by a parabola [Fig. 2(a)], so $v_y(t)$ decreases linearly in time [Fig. 2(b)]. Further, the acceleration is proportional to the impact velocity, as the inset in Fig. 2(b) illustrates: $a_y = \alpha v_0 g$, where the slope of the line gives $\alpha = 0.0064 \pm 0.0001$ s/cm. Thus, the projectile slows almost to a stop in a time $t = 1/\alpha g \simeq 0.15$ s, independent of v_0. The projectile does not immediately come to a complete stop; rather it then moves very slowly downward over the next few seconds as the particles in the bed make small rearrangements in response to the collapse of the transient crater.

The drag force on the projectile, while constant on the average, exhibits large fluctuations, which have a f^{-2} spectrum (Fig. 3).

The simulation determines all of the forces on each particle at every instance of time. Every force exerted by a particle on the projectile during a short portion of its travel is shown in Fig. 4. At each point in the projectile's trajectory only a few particles exert a significant force on the projectile. Each peak in the magnitude of the force between an individual particle and the projectile in Fig. 4 corresponds to a maximum force felt by the first particle in a force chain [18] that extends downward. Each force chain consists of a string of particles in contact. The sum of the magnitudes of forces felt by each particle in this chain is much greater than the average for the particles in the bed, as can be seen in Fig. 1 (simulation), where dark chains of particles extend downward from the projectile into the particle bed.

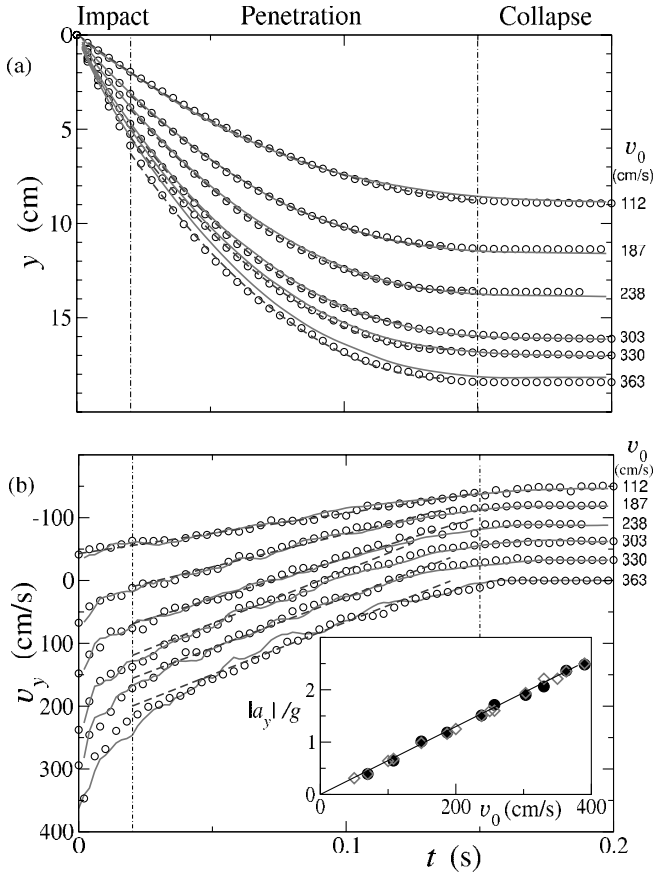

FIG. 2. (a) Position $y(t)$ and (b) velocity $v_y(t)$ of the projectile as a function of time for different impact velocities, from both experiment (○) and simulation (solid lines). The two vertical dot-dashed lines give approximate boundaries between three regions: impact, where the projectile rapidly decelerates (cf. Fig. 3); penetration, where the mean acceleration is constant, as illustrated by a dashed line fit in (a) of a parabola to the results from experiment and simulation for each v_0; and collapse, where the projectile has almost stopped and the particles above it are collapsing to fill the transient crater left by the penetration. The ordinate for (b) for each successive impact velocity $v_0 < 363$ cm/s is shifted by 30 cm/s for clarity. Inset: normalized acceleration of the projectile versus impact velocity from experiment (●) and simulation (◇).

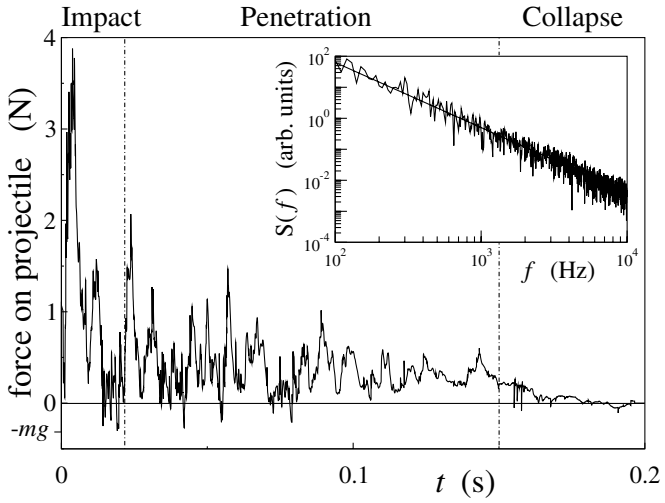

FIG. 3. The time series of the force on the projectile obtained from the simulation. The three regimes of motion are separated by dot-dashed lines. Inset: the power spectrum of the projectile acceleration during the penetration regime (0.02–0.15 s) for a projectile with initial velocity $v_0 = 238$ cm/s is described by $f^{-\alpha}$ with $\alpha = 2.1 \pm 0.2$.

Results for the probability distribution $P(F, t)$ of all normal forces between particles located in front of the projectile in a semicircular region of radius $1.5D$ centered at the bottom-most point of the projectile are shown in Fig. 5. The distribution $P(F, t)$ changes with time during impact but is time invariant during penetration: Fig. 5 shows the same distribution at times t_2 and t_3, which are, respectively, early and late in the penetration regime. The presence of an inflection point F^* in $P(F, t)$ marks the beginning of exponential decay for large F. The crossover to an exponential distribution at F^* increases linearly with v_0, as shown in the inset of Fig. 5. After the projectile has almost stopped, the distribution is similar to that found in previous studies of equilibrium [19] and near equilibrium [20] force distributions.

Discussion.—Our experiments and simulations show that the mean drag force on a projectile dropped into a granular medium is constant during most of the projectile's trajectory, and this drag force is proportional to the projectile's impact velocity. In our experiments inertia plays a major role. Interestingly, previous experiments with low constant velocities and negligible inertial effects also yielded a constant drag force in a granular medium [21].

Since the deceleration of the projectile is proportional to the impact velocity [see the inset in Fig. 2(b)], the projectile penetration depth is also proportional to the impact velocity. While our results are for a two-dimensional system, the linear dependence of the penetration depth on impact velocity has recently also been observed for projectile impact in a three-dimensional granular medium [22].

The drag force on our projectile fluctuates strongly, as found also for cylinders dragged at small constant velocities in experiments ($v \simeq 0.1$ cm/s) [21] and simulations ($v \simeq 2$ cm/s) [9,23,24]. The power spectrum of the force fluctuations has a f^{-2} dependence, as observed

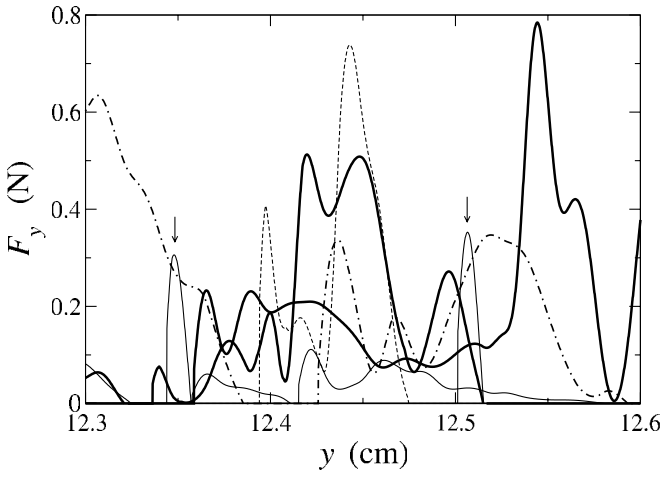

FIG. 4. Vertical component of the force computed for *every* particle in contact with the projectile during part of the penetration regime ($0.100 < t < 0.108$ s in Figs. 2 and 3). Each force grows, reaches a maximum (representing the inclusion of a particle in a particular force chain), and then decreases. Each type of line represents a particular particle; thus, the two arrows correspond to the *same* particle that appeared first at 12.344 cm and then reappeared at 12.501 cm. The projectile impact velocity was $v_0 = 238$ cm/s. The average of the y component of the force on the projectile during this interval was 0.57 N.

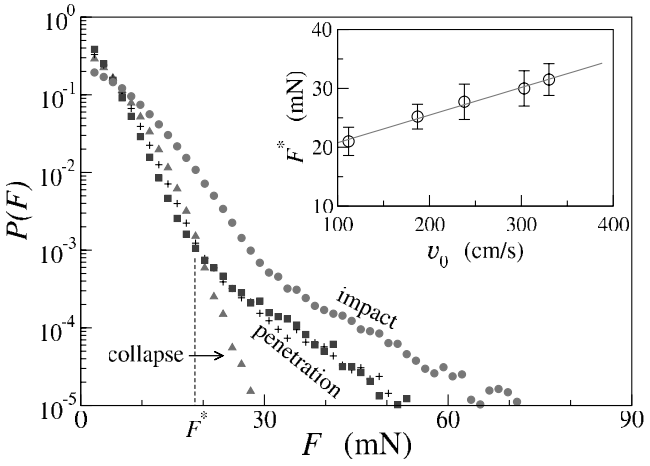

FIG. 5. Probability distribution of normal contact forces between grains for a projectile with $v_0 = 112$ cm/s at the following times: during impact ($t_1 = 0.02$ s, ●), early in the penetration regime ($t_2 = 0.05$ s, ■), late in the penetration regime ($t_3 = 0.12$ s, +), and during collapse ($t_4 = 0.20$ s, ▲). The distribution decays exponentially for $F > F^*$. The dependence of F^* on the impact velocity is shown in the inset; the slope is 0.047 ± 0.004 mN s/cm. Each curve was obtained by averaging over 50 runs.

in measurements of fluctuations of the stress on a slowly sheared two-dimensional granular medium [25] and in measurements of the torque on a torsional pendulum in contact with a vibrofluidized granular bed [26]. The f^{-2} dependence is explained by assuming random jumps in the drag force [25]. In our experiment these jumps originate from the variation of the forces exerted by the grains in contact with the projectile (Fig. 4).

Finally, our simulations have yielded the normal contact forces for all particles in the bed. The distribution function for the forces on the particles in front of the projectile rapidly evolves immediately after the projectile makes contact with the bed, and then the distribution becomes stationary as the projectile penetrates the bed. This stationary distribution decays exponentially beyond an inflection point at F^* whose value is linearly proportional to the impact velocity. This is the first determination of the force distribution for a granular medium for an accelerating particle. During impact, our force distribution is different from that measured for static beds [19], where the force distribution decayed exponentially at all times, as predicted by the q model [27].

We thank John de Bruyn and W. D. McCormick for their helpful comments and suggestions. This work was supported by the Engineering Research Program of the Office of Basic Energy Sciences of the U.S. Department of Energy (Grant No. DE-FG03-93ER14312), by the Texas Advanced Research Program, and by the Office of Naval Research Quantum Optics Initiative. M. P. C. gratefully acknowledges the support of the Italian-Fulbright commission.

*Electronic address: picaciamarra@na.infn.it
†Electronic address: swinney@chaos.utexas.edu

[1] D. J. Roddy, R. O. Pepin, and R. B. Merrill, *Impact and Explosion Cratering* (Pergamon Press, New York, 1977).
[2] H. Mizutani, S. Kawakami, Y. Takagi, M. Kato, and M. Kumazav, in *Proceedings of the 30th Lunar and Planetary Science Conference* [J. Geophys. Res. A 88, 835 (1983)].
[3] H. J. Melosh, *Impact Cratering: A Geologic Process* (Oxford University Press, New York, 1989).
[4] S. T. Thoroddsen and A. Q. Shen, Phys. Fluids **13**, 4 (2001).
[5] R. Mikkelsen, M. Versluis, E. Koene, G.W. Bruggert, D. vam der Meer, and D. Lohse, Phys. Fluids **14**, S14 (2002).
[6] J. S. Uehara, M. A. Ambroso, R. P. Ojha, and D. J. Durian, Phys. Rev. Lett. **90**, 194301 (2003).
[7] A. M. Walsh, K. E. Holloway, P. Habdas, and J. R. de Bruyn, Phys. Rev. Lett. **91**, 104301 (2003).
[8] J. C. Crocker and D. G. Grier, J. Colloid Sci. **179**, 298 (1996).
[9] V. Buchholtz and T. Pöschel, Granular Matter **1**, 33 (1998).
[10] N. V. Brilliantov, F. Spahn, J. M. Hertzsch, and T. Pöschel, Phys. Rev. E **53**, 5382 (1996).
[11] As in most other MD simulations of granular media with a soft-core potential (e.g., [12,13]), we use a value of k that is far smaller than the physical value (10^6 kg s^{-2} for nylon) because a higher value is computationally too expensive; the integration time must have the form $\delta t \propto k^{-1/2}$ for collisions to be modeled effectively [14]. The success of past [12,13] and present MD simulations with a small value of k indicates that the model, despite this flaw, captures much of the dissipative dynamics.
[12] L. E. Silbert, D. Ertas, G. S. Grest, T. C. Halsey, D. Levine, and S. J. Plimpton, Phys. Rev. E **64**, 051302 (2001).
[13] D. C. Rapaport, Phys. Rev. E **65**, 061306 (2002).
[14] J.W. Landry, G. S. Grest, L. E. Silbert, and S. J. Plimpton, Phys. Rev. E **67**, 041303 (2003).
[15] L. Labous, A. D. Rosato, and R. N. Dave, Phys. Rev. E **56**, 5717 (1997).
[16] P. A. Cundall and O. D. L. Strack, Geotechnique **29**, 47 (1979).
[17] J.W. Glaheen and T. A. McMahon, Phys. Fluids **8**, 2078 (1996).
[18] I. Albert, P. Tegzes, B. Kahng, R. Albert, J. G. Sample, M. Pfeifer, A. L. Barabási, T. Vicsek, and P. Schiffer, Phys. Rev. Lett. **84**, 5122 (2000).
[19] D. L. Blair, N.W. Mueggenburg, A. H. Marshall, H. M. Jaeger, and S. R. Nagel, Phys. Rev. E **63**, 041304 (2001).
[20] D.W. Howell, R. P. Behringer, and C. T. Veje, Chaos **9**, 559 (1999).
[21] R. Albert, M. A. Pfeifer, A. L. Barabási, and P. Schiffer, Phys. Rev. Lett. **82**, 205 (1999).
[22] J. R. de Bruyn and A. M. Walsh, Can. J. Phys. (to be published).
[23] C. Nouguier, C. Bohatier, J. J. Moreau, and F. Radjai, Granular Matter **2**, 171 (2000).
[24] For a projectile penetrating a dilute granular medium at high velocity ($v > 10^2$ cm/s) [9], much smaller fluctuations than we observe have been found.
[25] B. Miller, C. O'Hern, and R. P. Behringer, Phys. Rev. Lett. **77**, 3110 (1996).
[26] G. D'Anna and G. Gremaud, Nature (London) **413**, 407 (2001).
[27] S. N. Coppersmith, C. H. Liu, S. Majumdar, O. Narayan, and T. A. Witten, Phys. Rev. E **53**, 4673 (1995).